Illuminating the nature and behavior of the active center

The key for photocatalytic H_2 production in Co@NH_2-MIL-125(Ti)

Iglesias-Juez, Ana; Castellanos, Sonia; Monte, Manuel; Osadchii, Dmitrii; Agostini, Giovanni; Nasalevich, Maxim A.; Santaclara, Jara G.; Olivos Suarez, Alma I.; Veber, Sergey L.; Fedin, Matvey V.

DOI
10.1039/c8ta05735d

Publication date
2018

Document Version
Final published version

Published in
Journal of Materials Chemistry A

Journal of Materials Chemistry A

COMMUNICATION

View Article Online
View Journal | View Issue

Cite this: J. Mater. Chem. A, 2018, 6, 17318

Received 15th June 2018
Accepted 16th August 2018

DOI: 10.1039/c8ta05735d

rsc.li/materials-a

Illuminating the nature and behavior of the active center: the key for photocatalytic H_2 production in Co@NH_2-MIL-125(Ti)†

Ana Iglesias-Juez, *[a] Sonia Castellanos, *[b] Manuel Monte,[c] Giovanni Agostini, ‡[c] Dmitrii Osadchii,[d] Maxim A. Nasalevich,[d] Jara G. Santaclara,[d] Alma I. Olivos Suarez, [d] Sergey L. Veber,[e] Matvey V. Fedin [e] and Jorge Gascón [df]

Advanced atomically resolved characterization methods unveil the mechanism of a promising photocatalytic Co@MOF(Ti) system for H_2 production. The combination of X-ray absorption spectroscopy (XAS) and electron paramagnetic resonance (EPR) experiments allows for the characterization of atomic and electronic rearrangements in the photoinduced species. This information provides the basis for the optimization of photocatalyst design.

The nanoporous nature of metal–organic frameworks (MOFs) does not only endow these materials with a large surface area but also with the possibility of confining active functionalities within their pores. This approach has proved successful for the design of photocatalytic composites where the MOF acts both as a photosensitizer and support.[1–5]

The first example of a ship-in-a-bottle protocol by Nasalevich *et al.* aimed at combining the advantages of homogeneous and heterogeneous catalysts by encapsulating a molecular cobalt-based hydrogen evolution catalyst in a titanium-based MOF (NH_2-MIL-125(Ti)).[6] This so-called Co@MOF system exhibited a 20-fold enhanced activity compared to the pristine NH_2-MIL-125(Ti). This protocol was later imitated with different cobalt complexes by Li *et al.*,[2] yielding an even larger increase in activity compared to the unloaded MOF.

It is generally assumed that the MOF scaffold absorbs the incident photons and then transfers electrons to the catalytic guests.[1] Outside the field of MOFs, the few examples of photocatalysts for the hydrogen evolution reaction (HER) based on TiO_2 materials doped with Co species assign to Co the role of a co-catalyst that receives electrons from the photoexcited TiO_2, thus slowing down charge recombination.[7,8] However, it is still challenging to experimentally probe the molecular and the valence electronic structures of these complex systems due to the low loadings and the heterogeneity of the active sites.

Understanding the interaction between the two metallic components in Co@MOF(Ti) materials (this is: the Ti-octamer cluster in the MOF and the Co-site hosted inside the MOF) during the catalytic cycle is thus of major importance to unravel the mechanism of photon-induced hydrogen production and, ultimately, to optimize their photocatalytic performance. These investigations are particularly important for the development of sustainable solar light-driven energy sources, given the green character of a photocatalyst that uses visible light and is based on inexpensive earth-abundant and non-toxic elements such as Ti and Co.

X-ray absorption spectroscopy (XAS) is a powerful technique for probing the local atomic structure around the absorbing atom, as well as the chemical state (oxidation and often spin state) of the catalytic center thanks to its element selectivity and sensitivity to the electronic structure. By using time-resolved XAS, the direct determination of the chemical state of the active site during catalytic conditions is made possible, allowing clarification of the mechanisms of catalyzed reactions.[9–12] Here, an *in situ* XAS study sheds light on the structure of the encapsulated cobalt species and on mechanistic aspects of the Co@MOF(Ti) multifunctional composite, providing an interpretation of the cooperative action between the photoactive MOF matrix and the catalytically active guest. The changes in the active sites were monitored during a pre-catalysis incubation period and during photocatalytic H_2 production, thus yielding a detailed time-

[a]Instituto de Catálisis y Petroleoquímica, CSIC, 28049 Madrid, Spain. E-mail: ana.iglesias@icp.csic.es

[b]Advanced Research Center for Nanolithography, 1090 BA Amsterdam, The Netherlands. E-mail: s.castellanos@arcnl.nl

[c]European Synchrotron Radiation Facility, 38000 Grenoble, Cedex 9, France

[d]Catalysis Engineering, Applied Sciences, Delft University of Technology, Julianalaan 136, 2628 BL, Delft, The Netherlands

[e]International Tomography Center SB RAS, Novosibirsk State University, Novosibirsk 630090, Russia

[f]King Abdullah University of Science and Technology, KAUST Catalysis Center, Advanced Catalytic Materials, Thuwal 23955, Saudi Arabia

† Electronic supplementary information (ESI) available: Photo-cell design for XAS experiments. Experimental conditions and XAS and EPR results. See DOI: 10.1039/c8ta05735d

‡ Present addresses: Leibniz-Institut für Katalyse e. V. an der Universität Rostock, Albert-Einstein-Strasse 29a, D-18059 Rostock, Germany.

resolved characterization of the electronic and structural behavior of the system. This is the first example of XAS measurements performed on a MOF-based system to study the photocatalytic sites under *operando* conditions.

X-ray absorption near edge spectroscopy (XANES) spectra were recorded for the freshly suspended Co@MOF sample and during its *in situ* incubation in acetonitrile/triethylamine/water (AN/TEA/H_2O 5 : 1 : 0.1). The initial and final Co K-edge XANES spectra, displayed in Fig. 1, indicate the presence of Co(II) species in both cases, as inferred from the edge position analysis.[13,14] A comparison with appropriate references (see Fig. S2†) shows analogous surrounding local symmetries, likely an octahedral first coordination environment. The spectra clearly differ from those obtained for the isolated Co(III)–cobaloxime complex (Fig. S3†). This complex was expected to be formed in the pores through the diffusion of the linear oxime ligand into the MOF before the addition of the Co(II) cations as dissolved $CoBr_2$. The diffusion of Co(II) ions was followed by their oxidation into Co(III) under O_2 flux.[6] The weak intensity of Co(II) Electron Paramagnetic Resonance (EPR) signals found for the fresh catalyst in the dark[6] seemed to support the assumption that most Co atoms resided in an EPR-silent Co(III) state. However, the new XANES data reveal that the existing species is Co(II), thus requiring re-investigation of the catalyst structure.

To gain more insight into the nature of the Co species in Co@MOF, the local structure around the Co atoms was studied by extended X-ray absorption spectroscopy (EXAFS). The Fourier transforms of the Co k^2-weighted spectra and the structural parameters determined from the curve-fitting are shown in Fig. 2 (complementary information in Fig. S4 and Table S1†). The EXAFS data of the Co@MOF catalyst clearly differ from those of both $CoBr_2$ and Co-oxime references (Fig. S5†).[13–16] The fitting suggests that the Co(II) species initially present an octahedral first coordination sphere formed by O and/or N atoms around 2 Å and also a small contribution of Br neighbors. O and N light scatterers are difficult to distinguish in the EXAFS fitting (as can be derived from the evolution of scattering amplitude and phase shift functions with Z number).[17,18]

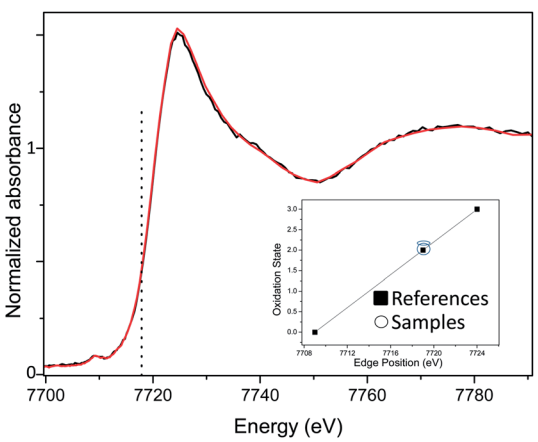

Fig. 1 XANES spectra of the freshly suspended Co@MOF (black) and after *in situ* AN/TEA/H_2O incubation (red).

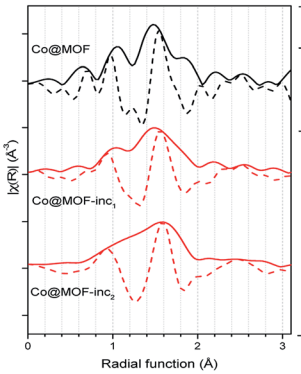

Co@MOF				
Coord. shell	fresh		Incubated$_2$	
	N	R(Å)	N	R(Å)
Co-O	5.9(9)	2.14(4)	3.8(2)	2.05(2)
Co-N	-	-	1.5(3)	1.93(1)
Co-Br	0.5(3)	2.45(3)	-	-
Co-Co	0.8(4)	3.39(5)	0.2(2)	2.84(3)
Co-Ti	-	-	0.8(2)	3.08(2)

Fig. 2 Left: k^2-Weighted modulus and real part of the Fourier transform of Co K-edge EXAFS spectra corresponding to Co@MOF before (black) and after incubation periods (red): $inc_1 = 12$ h and $inc_2 = 24$ h. Right: Structural parameters derived from EXAFS analysis (numbers between parenthesis are the errors in the last digit shown).

However, participation of N atoms in the coordination of Co is supported by previously reported IR spectroscopy results, where the emergence of red-shifted N–H stretching bands was detected for Co@MOF in comparison with the empty MOF.[6] A Co–Co atomic distance of a second coordination shell is detected at 3.4 Å, suggesting the initial presence of Co dimers.[19,20]

The results of the EXAFS fitting show that the Co local environment evolves during the incubation period in AN/TEA/H_2O. Specifically, after 12 h of incubation, an increase of the Co–N distance seems to occur together with a decrease in Co–Co coordination number and the appearance of more scatterers in second–third coordination spheres. After 24 h, these differences are more obvious in the normalized Fourier transforms (Fig. 2). On the one hand, near absence of the second coordination shell Co–Co (coordination number < 0.3) is observed; on the other hand, it can be seen that the shape of the modulus and real part of the 24 h incubated sample is significantly different from both the fresh system and from the 12 h incubation, in the region between 2.0 and 3.2 Å. The comparison between normalized Fourier transforms could indicate the presence of metal–MOF wall interface contributions. Thus, it is required to introduce another coordination shell, Co–Ti, at longer distances ($R = 3.1$ Å) to obtain a good fitting of the data (Fig. 2 right). All these changes point out a reorganization of the Co-species in the pores when treated with the AN/TEA/H_2O mixture.

EXAFS fitting results on Co@MOF upon incubation with AN/TEA/H_2O therefore suggest the presence of Co-monomers bonded to the Ti-cluster through oxygen atoms and to either $-NH_2$ residue in the MOF organic linker or N atoms of the oxime ligand. The presence of the linear oxime ligands inside the pores could prevent oligomerization processes, due to steric impediment. This could mediate the stabilization of a Co complex connected to the Ti oxo-cluster of the MOF through its coordination with N atoms from the ligand. In view of the XANES and EXAFS results, a structural model of the Co centers in the Co@MOF system is proposed (Fig. 3).

The presence of Co(II) species in the form of O-bridged dimers that dissociate upon incubation can explain previous EPR results.[6]

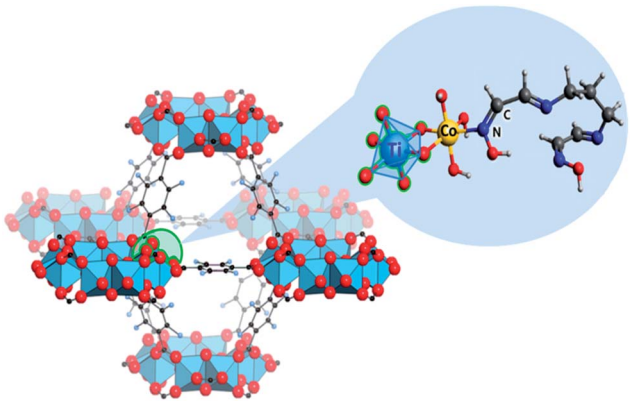

Fig. 3 Proposed model, extracted from EXAFS fitting data, for the active Co centers in the Co@MOF system.

In such dimers, metal ions are typically coupled by a strong antiferromagnetic exchange in the order of 100–200 K [21,22] and therefore at $T < 50$ K they become EPR silent. Indeed, the freshly suspended sample, before illumination, shows only a weak signal at $g \sim 4$, which is assigned to residual Co(II) in the high spin state. The photogeneration of a new signal at the $g \sim 2$ region on the timescale of 10–20 hours is compatible with incubation and electron transfer reactions occurring in parallel. The photoinduced EPR signal shows several remarkable features. It has a closely Gaussian line shape at X/Q-bands with peak-to-peak width ~300 mT, but the apparent g-values differ at the X- and Q-band, being ~2.65 and ~2.23, respectively (Fig. 4 and S8†). The intensity of this signal drastically grows with temperature, whereas the shape remains closely the same (Fig. 4 and S8†).

These observations can be assigned to an exchange-narrowed cluster/network of magnetically coupled ions with noticeable distribution of structural parameters. The exchange coupling is clearly antiferromagnetic, and we can estimate its effective value J_{eff} by fitting the temperature dependence of signal intensity with a Boltzmann function $\exp(-J_{eff}/kT)$, giving $J_{eff} = 250 \pm 50$ K (Fig. 4). Such large values of exchange coupling assume rather short distances between paramagnetic centers in the cluster, allowing us to assume oxo-bridging.[21,22] The clusters/networks can include both Co(II) ions and photoinduced Ti(III) ions. Upon prolonged illumination, the number of Ti(III) ions might exceed the number of Co(II) ions, therefore the properties of exchange clusters should be dominated by those of Ti(III). Indeed, we were able to detect the photoinduced EPR signal of Co@MOF up to nearly room temperatures, which is not common for fast-relaxing cobalt species, but is more plausible for slower-relaxing $3d^1$ Ti(III) species. Thus, the X/Q-band variable-temperature EPR study supports the formation of antiferromagnetically coupled exchange clusters/networks of Co(II) and Ti(III) ions upon illumination of Co@MOF in the reaction mixture, where the dominant exchange coupling occurs between closely located pairs of ions, possibly connected *via* the oxo-bridge.

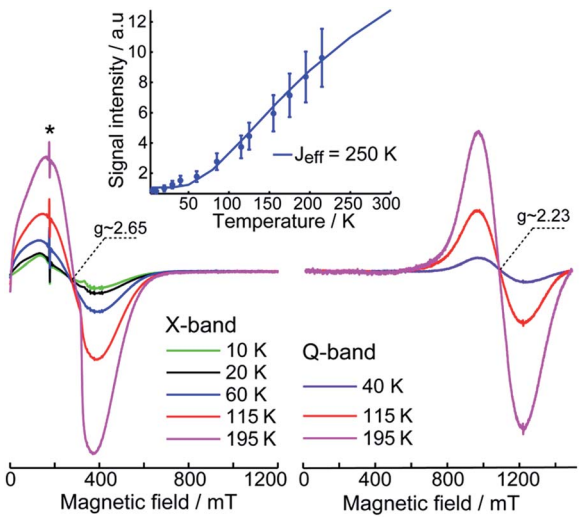

Fig. 4 Variable-temperature X/Q-band EPR spectra of Co@MOF in $CH_3CN/TEA/H_2O$, which was exposed to 380 nm light irradiation for 19 h prior to measurements. Asterisk marks the reference signal used for normalization of X-band spectra. Inset: signal intensity *vs.* temperature and the fit.

It should be noted that such participation of Ti in the heterometallic active site is crucial for the boosting of the catalytic activity. When the same protocol to diffuse Co(II) was applied onto a Zr-based and an Al-based MOF featuring the same aminoterephthalate ligands and similar absorption range, the so-called NH_2-UiO-66(Zr) and NH_2-MIL-53(Al),[23] respectively, the resulting Co-loaded MOFs did not yield any catalytic activity (ESI Fig. S10†). The lack of activity in these systems further supports that the sole encapsulation of Co(II) in a network that can absorb visible light cannot yield the suitable photocatalytic sites and that the Ti nodes in the MOF contribute to them.

Operando XANES experiments were performed to further investigate how light induced the catalytic activity in Co@MOF. Differential mode analysis of Co K-edge (see the ESI† for more details) provides information about the metal properties together with the charge localization process upon photoexcitation (Fig. 5). The illumination of the suspension with visible light in the reaction media induced a shift of the XANES edge toward lower energies (green features). The shift was accompanied by a concomitant decrease in the white line intensity and the shoulder around 7737 eV, attributed to an electron density increase of the p and d states, respectively, involved in the 1s–4sp and 1s–3d resonance transitions (orange features).

Therefore, the results point to a partial reduction of the Co(II) centers[24] by charge transfer directly into p and d(e_g) states.

These changes became more evident after 5 h, in line with the activation period induced by illumination previously reported for this system[6] and proved to be reversible after the light was switched off, as well as reproducible upon a second light exposure cycle (Fig. 5). Therefore, photoinduced charge transfer reaches a photostationary state and reverts to the original situation in the absence of light, which indicates that the electrons accumulated in the Co-sites electronically coupled to the Ti atoms of the MOF platform are used for photocatalytic water reduction in a reversible manner. Many studies in the literature investigated if Co-based hydrogen evolution catalysts require

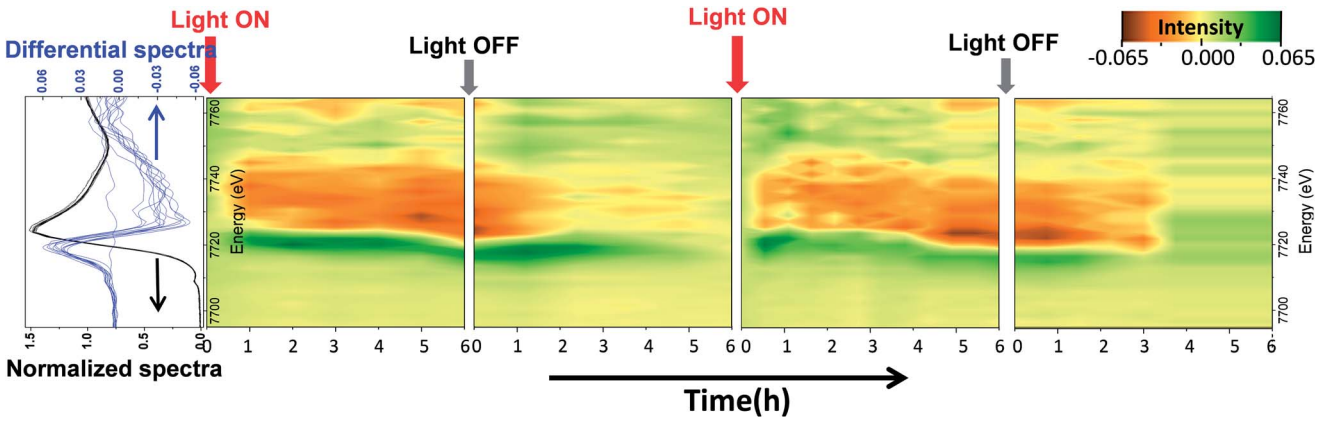

Fig. 5 Intensity contour map of normalized differential XANES spectra during cycles of light switching for Co@MOF in AN/TEA/H_2O solution.

the formation of Co(I) intermediates for water reduction.[25–29] This work shows that a partial reduction of Co centres takes place by charge transfer and these reduced species are the active centres for H_2 formation, but a total reduction to Co(I) does not occur.

Conclusions

In summary, XANES and EXAFS analyses unveil the structure and properties of the promising photocatalytic system Co@NH_2-MIL-125(Ti) together with the charge localization process after photo-excitation. The results indicate that during the incubation period Co-dimers in this composite partially dissociate and bring Co(II) species closer to the Ti-clusters. In this configuration, visible light promotes the partial reduction of the Co(II)-sites, which are the active catalytic centers responsible for hydrogen evolution. This configuration is in line with the observed evolution of the EPR spectra upon illumination of Co@MOF, where the registered broad signal in the photostationary state is indicative of the electronic coupling between Co and Ti. Thus, while the linear oxime ligand does not seem to promote the formation of the previously proposed cobaloxime in the pores, its function might favor the dispersion of the Co(II) cations and enable the formation of Co-sites with monomeric configuration that can connect to the Ti-oxoclusters of the MOF in the active state.

Conflicts of interest

There are no conflicts to declare.

Acknowledgements

A. I. J. acknowledges financial support from the CSIC (PIM-2014 201480I012 project). S. L. V. and M. V. F. thank the Russian Science Foundation (No. 14-13-00826) for supporting the EPR studies. We are grateful to the ESRF for granting beamtime at BM23, as well as the staff members of the station for their help during the measurements. We also would like to thank Ruud van Tol from Delft mechanical workshop for all his support during the design of the XAS experimental cell.

Notes and references

1 S. Pullen and S. Ott, *Top. Catal.*, 2016, **59**(19), 1712–1721.
2 Z. Li, J. D. Xiao and H. L. Jiang, *ACS Catal.*, 2016, **6**(8), 5359–5365.
3 W. Wang, X. Xu, W. Zhou and Z. Shao, *Adv. Sci.*, 2017, **4**, 1600371.
4 S. Wang and X. Wang, *Small*, 2015, **11**(26), 3097–3112.
5 Y. Fu, H. Yang, R. Du, G. Tu, C. Xu, F. Zhang, M. Fan and W. Zhu, *RSC Adv.*, 2017, **7**(68), 42819–42825.
6 M. A. Nasalevich, R. Becker, E. V. Ramos-Fernandez, S. Castellanos, S. L. Veber, M. V. Fedin, F. Kapteijn, J. N. H. Reek, J. I. van der Vlugt and J. Gascon, *Energy Environ. Sci.*, 2015, **8**, 364–375.
7 X. Yue, S. Yi, R. Wang, Z. Zhang and S. Qiu, *Small*, 2017, **13**, 1603301.
8 L. Mahoney, R. Peng, C. M. Wu, J. Baltrusaitis and R. T. Koodali, *Int. J. Hydrogen Energy*, 2015, **40**(34), 10795–10806.
9 S. Bordiga, F. Bonino, K. Petter Lillerudb and C. Lamberti, *Chem. Soc. Rev.*, 2010, **39**, 4885–4927.
10 D. Moonshiram, C. Gimbert-Suriñach, A. Guda, A. Picon, C. S. Lehmann, X. Zhang, G. Doumy, A. Mariearch, J. Benet-Buchholz, A. Soldatov, A. Llobet and S. H. Southworth, *J. Am. Chem. Soc.*, 2016, **138**, 10586–10596.
11 X. B. Li, Y. J. Gao, Y. Wang, F. Zhan, X. Y. Zhang, Q. Y. Kong, N. J. Zhao, Q. Guo, H. L. Wu, Z. J. Li, Y. Tao, J. P. Zhang, B. Chen, C. H. Tung and L. Z. Wu, *J. Am. Chem. Soc.*, 2017, **139**, 4789–4796.
12 G. Smolentsev, B. Cecconi, A. Guda, M. Chavarot-Kerlidou, J. A. van Bokhoven, M. Nachtegaal and V. Artero, *Chem.–Eur. J.*, 2015, **21**, 15158–15162.
13 C. Maurizio, N. El Habra, G. Rossetto, M. Merlini, E. Cattaruzza, L. Pandolfo and M. Casarin, *Chem. Mater.*, 2010, **22**(5), 1933–1942.

14 P. A. O'day, G. A. Parks Jr and G. E. Brown, *Clays Clay Miner.*, 1994, **42**(3), 337–355.
15 M. Sano, T. Maruo, Y. Masuda and H. Yamatera, *J. Solution Chem.*, 1986, **15**(10), 803–809.
16 M. Giorgetti, M. Berrettoni, I. Ascone, S. Zamponi, R. Seeber and R. Marassi, *Electrochim. Acta*, 2000, **45**, 4475–4482.
17 G. Tolkiehn, P. Rabe and A. Werner, *Inner-Shell and X-Ray Physics of Atoms and Solids. Physics of Atoms and Molecules*. Springer, Boston, MA, 1981, pp. 675–678.
18 A. Murrai and A. R. Chetal, *Phys. Status Solidi B*, 1994, **183**, 287–290.
19 F. A. Cotton and R. C. Elder, *Inorg. Chem.*, 1965, **4**(8), 1145–1151.
20 C. Bresson, S. Esnouf, C. Lamouroux, P. L. Solari and C. Den Auwer, *New J. Chem.*, 2006, **30**(3), 416–424.
21 J. W. Dawson, H. B. Gray, H. Eckhardt Hoenig, G. R. Rossman, J. M. Schredder and R.-H. Wang, *Biochemistry*, 1972, **11**, 461–465.
22 L. Petersson, A. Graslund, A. Ehrenberg, B.-M. Sjdberg and P. J. Reichard, *Biol. Chem.*, 1980, **255**, 6706–6712.
23 M. A. Nasalevich, C. H. Hendon, J. G. Santaclara, K. Svane, B. van der Linden, S. L. Veber, M. V. Fedin, A. J. Houtepen, M. A. van der Veen, F. Kapteijn, A. Walsh and J. Gascon, *Sci. Rep.*, 2016, **6**, 23676.
24 G. Smolentsev, A. A. Guda, M. Janousch, C. Frieh, G. Jud, F. Zamponi, M. Chavarot-Kerlidou, V. Artero, J. A. van Bokhoven and M. Nachtegaal, *Faraday Discuss.*, 2014, **171**, 259–273.
25 W. T. Eckenhoff, W. R. McNamara, P. Du and R. Eisenberg, *Biochim. Biophys. Acta, Bioenerg.*, 2013, **1827**, 958–973.
26 P. Jacques, V. Artero and J. Pécaut, *Proc. Natl. Acad. Sci. U. S. A.*, 2009, **106**, 20627–20632.
27 D. C. Lacy, G. M. Roberts and J. C. Peters, *J. Am. Chem. Soc.*, 2015, **137**, 4860–4864.
28 Z. J. Li, F. Zhan, H. Xiao, X. Zhang, Q. Y. Kong, X. B. Fan, W. Q. Liu, M. Y. Huang, C. Huang, Y. J. Gao, X. B. Li, Q. Y. Meng, K. Feng, B. Chen, C. H. Tung, H. F. Zhao, Y. Tao and L. Z. Wu, *J. Phys. Chem. Lett.*, 2016, **7**, 5253–5258.
29 G. Smolentsev, A. Guda, X. Zhang, K. Haldrup, E. S. Andreiadis, M. Chavarot-Kerlidou, S. E. Canton, M. Nachtegaal, V. Artero and V. Sundstrom, *J. Phys. Chem. C*, 2013, **117**, 17367–17375.

